An Interpolation Scheme for Green's Function and its Application in Method of Moment

Yanlin Xu [1], Hu Yang [1], Xiang Liu [2], and Rongjun Shen [1]

[1] College of Electronic Science
National University of Defense Technology, Changsha, 410073, China
13298656824@163.com, yanghu90@163.com, 271069796@qq.com

[2] College of Information and Communication Engineering
Hunan Institute of Science and Technology, Yueyang, 414000, China
1175235011@qq.com

Abstract ─ An interpolation scheme is put forward to accelerate the calculation of free space Green's function. Through theoretical analysis, a universal rule on how to build value lists for the phase item of Green's function is discussed. And this rule can guarantee accuracy of the interpolation scheme. Accuracy and efficiency of the scheme are verified in the calculation of impedance matrix for method of moment. Besides, this scheme can also be applied to other applications which contain the calculation of Green's functions and is especially useful for the analysis of large scale problems. Moreover, this scheme can be combined with other existing improved approaches of method of moment.

Index Terms ─ Green's function, impedance matrix, interpolation scheme, method of moment.

I. INTRODUCTION

Green's function of free space can be viewed as the electric field of ideal point source. Thus, it is the basis of electromagnetic problems and is frequently used in computational electromagnetics [1-4]. In this work, a typical application of Green's function in method of moment (MoM) is discussed.

MoM is a classic frequency-domain algorithm and was first applied to the analysis of electric field integral equation by Harrington in 1968 [5]. It transforms a vector integral equation into a scalar matrix equation by two processes called discretization and test.

The discretization process discretizes the unknown vector into a series of basic functions and the test process uses a series of test functions to make inner products. Usually, to ensure accuracy, a sampling rate of $\lambda/10$ is required. This makes MoM unsuitable for large scale problems due to the limitations on memory cost $O(N^2)$ and computational complexity $O(N^3)$.

To overcome or improve drawbacks of MoM and accelerate the calculation of its impedance matrix, several approaches are proposed in the past decades. Among which, fast multi-pole method (FMM) and multi-level fast multi-pole method (MLFMM) [6-8] attracts most attention due to its excellent performance in efficiency and accuracy. Apart from FMM/MLFMM, other improved approaches such as multilevel matrix decomposition algorithm (MLMDA) [9], wavelet-based modelling method [10], improved impedance matrix localization method (IML) [11], triangular expansion method [12], synthetic basis functions method (SBFM) [13] and etc. also made great progresses. To summarize, these improved approaches accelerate the calculation of impedance matrix through mathematical operation.

Unlike the above, in this work, we put emphasis on the calculation of Green's functions. As is known to all, the calculation of Green's function takes a considerable part in the calculation of impedance matrix for MoM. Then, considering periodic properties of phase term of Green's function, an interpolation scheme is presented to improve the efficiency of the calculation of Green's function. This work first discusses the calculation of impedance matrix and analyzes the proportion of Green's function in the total calculation. Then, based on the periodic properties of Green's function, a value list for the phase term is built to accelerate the calculation process. Moreover, we theoretically analyze and prove the determination of the number of segments for the value list to acquire a constant accuracy. Efficiency and accuracy of the interpolation scheme are validated by numerical examples in the calculation of impedance matrix for MoM. Notably, this scheme can also be perfectly combined other applications those contain the calculation of Green's function as it is an independent process.

II. BASIC THEORY

For PEC bodies, MoM usually bases on the EFIE, which can be compactly written as:

Submitted On: January 6, 2018
Accepted On: July 3, 2018

$$\hat{n}\times L(\boldsymbol{J})=\hat{n}\times \boldsymbol{E}_{inc}, \tag{1}$$

Where $\boldsymbol{E}_{inc}$ represents the incident wave, $\boldsymbol{J}$ is the surface current, L is the electric integral operator and defined as:

$$L(\boldsymbol{X})=j\omega\mu\int_S[\boldsymbol{X}+\frac{1}{k^2}\nabla(\nabla\cdot\boldsymbol{X})]gdS. \tag{2}$$

Usually, Rao-Wilton-Glisson (RWG) functions [14] are adopted to discretize (1) and transform it into a linear matrix equation:

$$ZI=V, \tag{3}$$

Where $Z=\{z_{mn}\}_{N\times N}$ is the impedance matrix, $V_{N\times 1}$ is the exciting matrix, and $I_{N\times 1}$ is the current coefficients matrix of RWG functions. The impedance matrix is calculated as (4).

Where $\boldsymbol{f}_m(\boldsymbol{r})$ is the m-th RWG function, g and k is the Green's function of free space and the wave number.

Equation (4) contains two parts which are computed in (5) and (6). Where $\boldsymbol{\rho}$ represents the vector in a couple of triangular patches $T_n^{\pm}$, l_n is the edge length of the common edge of $T_n^{\pm}$, $A_n^{\pm}$ is the areas of $T_n^{\pm}$. These symbols are the basic definitions of RWG function, and we are not going to introduce them for the sake of simplicity.

$$z_{mn}=\left\langle \boldsymbol{f}_m(\boldsymbol{r}),L(\boldsymbol{f}_n(\boldsymbol{r}'))\right\rangle=\int_s \boldsymbol{f}_m(\boldsymbol{r})\cdot L(\boldsymbol{f}_n(\boldsymbol{r}'))ds=j\omega\mu\int_s\int_{s'}g(\boldsymbol{r}-\boldsymbol{r}')\left(\begin{array}{c}\boldsymbol{f}_m(\boldsymbol{r})\cdot\boldsymbol{f}_n(\boldsymbol{r}')-\\ \frac{1}{k^2}\nabla_s\cdot\boldsymbol{f}_m(\boldsymbol{r})\nabla'_s\cdot\boldsymbol{f}_n(\boldsymbol{r}')\end{array}\right)ds'ds, \tag{4}$$

$$\int_s\int_{s'}g(\boldsymbol{r}-\boldsymbol{r}')\left(\boldsymbol{f}_m(\boldsymbol{r})\cdot\boldsymbol{f}_n(\boldsymbol{r}')\right)ds'ds=\left[\left(\int_{s_n}g(\boldsymbol{r}_{m,c}^{+}-\boldsymbol{r}')\boldsymbol{f}_n(\boldsymbol{r}')ds'\right)\cdot\left(\boldsymbol{f}_m(\boldsymbol{r}_{m,c}^{+})A_m^{+}\right)+\left(\int_{s_n}g(\boldsymbol{r}_{m,c}^{-}-\boldsymbol{r}')\boldsymbol{f}_n(\boldsymbol{r}')ds'\right)\cdot\left(\boldsymbol{f}_m(\boldsymbol{r}_{m,c}^{-})A_m^{-}\right)\right]$$

$$=\frac{l_nl_m}{4}\left(\frac{1}{A_n^{+}}\int_{T_n^{+}}\boldsymbol{\rho}_n^{+}g(\boldsymbol{r}_{m,c}^{+}-\boldsymbol{r}')ds'\cdot\boldsymbol{\rho}_m^{c+}+\frac{1}{A_n^{-}}\int_{T_n^{-}}\boldsymbol{\rho}_n^{-}g(\boldsymbol{r}_{m,c}^{+}-\boldsymbol{r}')ds'\cdot\boldsymbol{\rho}_m^{c+}+\frac{1}{A_n^{+}}\int_{T_n^{+}}\boldsymbol{\rho}_n^{+}g(\boldsymbol{r}_{m,c}^{-}-\boldsymbol{r}')ds'\cdot\boldsymbol{\rho}_m^{c-}+\frac{1}{A_n^{-}}\int_{T_n^{-}}\boldsymbol{\rho}_n^{-}g(\boldsymbol{r}_{m,c}^{-}-\boldsymbol{r}')ds'\cdot\boldsymbol{\rho}_m^{c-}\right), \tag{5}$$

$$=\frac{l_nl_m}{4}\left(g(\boldsymbol{r}_{m,c}^{+}-\boldsymbol{r}_{n,c}^{+})\boldsymbol{\rho}_n^{c+}\cdot\boldsymbol{\rho}_m^{c+}+g(\boldsymbol{r}_{m,c}^{+}-\boldsymbol{r}_{n,c}^{-})\boldsymbol{\rho}_n^{c-}\cdot\boldsymbol{\rho}_m^{c+}+g(\boldsymbol{r}_{m,c}^{-}-\boldsymbol{r}_{n,c}^{+})\boldsymbol{\rho}_n^{c+}\cdot\boldsymbol{\rho}_m^{c-}+g(\boldsymbol{r}_{m,c}^{-}-\boldsymbol{r}_{n,c}^{-})\boldsymbol{\rho}_n^{c-}\cdot\boldsymbol{\rho}_m^{c-}\right)$$

$$\int_s\int_{s'}g(\boldsymbol{r}-\boldsymbol{r}')\left(\nabla_s\cdot\boldsymbol{f}_m(\boldsymbol{r})\nabla'_s\cdot\boldsymbol{f}_n(\boldsymbol{r}')\right)ds'ds=l_m\left(\int_{s_n}\nabla'_s\cdot\boldsymbol{f}_n(\boldsymbol{r}')g(\boldsymbol{r}_{m,c}^{+}-\boldsymbol{r}')ds'-\int_{s_n}\nabla'_s\cdot\boldsymbol{f}_n(\boldsymbol{r}')g(\boldsymbol{r}_{m,c}^{-}-\boldsymbol{r}')ds'\right)$$

$$=l_ml_n\left(\frac{1}{A_n^{+}}\int_{T_n^{+}}g(\boldsymbol{r}_{m,c}^{+}-\boldsymbol{r}_{n,c}^{+})ds'-\frac{1}{A_n^{-}}\int_{T_n^{-}}g(\boldsymbol{r}_{m,c}^{+}-\boldsymbol{r}_{n,c}^{-})ds'-\frac{1}{A_n^{+}}\int_{T_n^{+}}g(\boldsymbol{r}_{m,c}^{-}-\boldsymbol{r}_{n,c}^{+})ds'+\frac{1}{A_n^{-}}\int_{T_n^{-}}g(\boldsymbol{r}_{m,c}^{-}-\boldsymbol{r}_{n,c}^{-})ds'\right). \tag{6}$$

From (5) and (6) we can see that, the calculation of Green's function takes a considerable part of the total calculation. For each Z_{mn}, Green's function needs to be calculated 4 times. Thus, for a problem with N RWG functions, the scale of impedance matrix will be N^2 which means Green's function need to be calculated $4N^2$ times. Moreover, considering the singularity of Green's function, if nine-point approximation [14] is adopted, the calculation of Green's function will be $36N^2$ times. Besides, (5) and (6) indicate the calculation of Green's function is independent of the calculation of impedance matrix. Thus, we can obtain the values of Green's functions in advance.

Green's function is defined as:

$$g(R)=e^{-jkR}/4\pi R. \tag{7}$$

For brevity, we ignore the constant coefficient of g and define $h=4\pi g$. h contains two parts: the magnitude item $1/R$ and the phase item e^{-jkR}. We plot the values of h changing with R, as shown in Fig. 1. From Fig. 1 we can see that values of h exhibit a periodic distribution around origin point with the decrease of R. And the periodic properties are caused by the phase item e^{-jkR}.

Considering trajectory of Green's function's phase item is a circle whose radius is 1. We can discretize the trajectory into numerous segments and build a value list for each segment, as shown in Fig. 2. With the value list, we no longer need to calculate the phase item and we can get the value directly from the list according to kR. Accuracy of the value list is controlled by the total number of segments M. And the larger of M, the higher accuracy it will be. To determine the proper number of segments M, we do the derivation for h:

$$\frac{dh}{dR}=(-\frac{1}{R^2}-\frac{jk}{R})e^{-jkR}. \tag{8}$$

Then,

$$|dh|=\sqrt{\frac{1}{R^4}+\frac{k^2}{R^2}}|dR|. \tag{9}$$

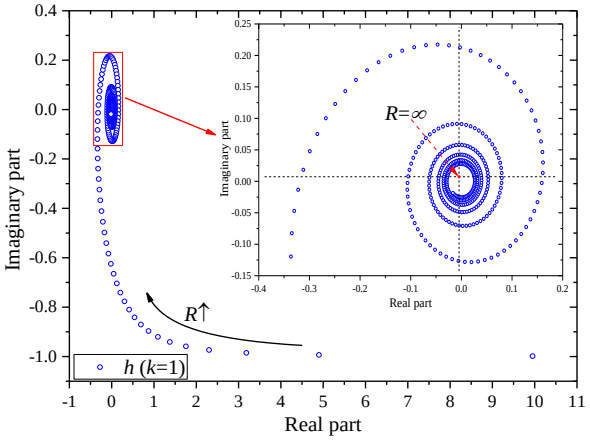

Fig. 1. Values of Green's function changing with R.

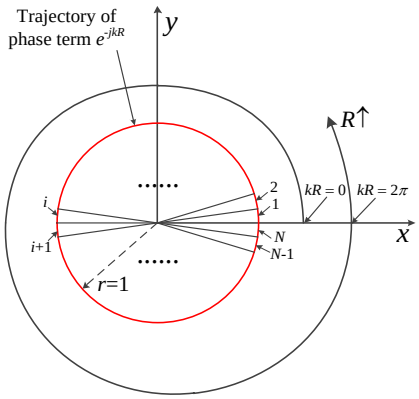

Fig. 2. Trajectory of Green's function phase item which is divided into N segments.

In fact, $|dh|$ represents the absolute error of h which is a circle around the real value as shown in Fig. 3 and accurate relationship between $|dh|$ and $|dR|$ is shown in Fig. 4.

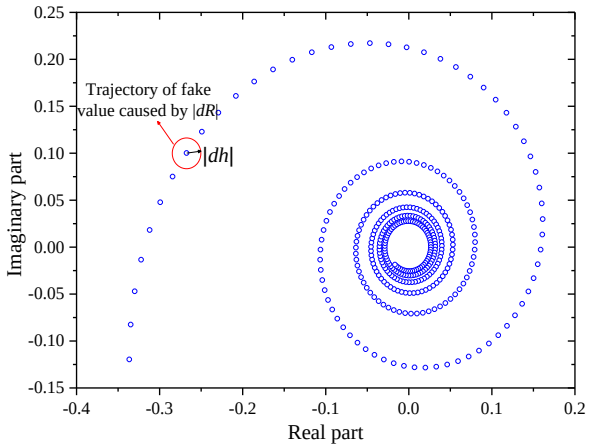

Fig. 3. Fake value trajectory of Green's function.

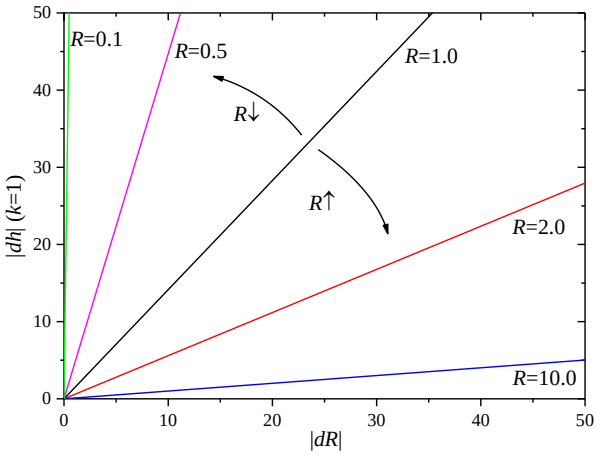

Fig. 4. Relationship between $|dh|$ and $|dR|$.

However, from (9) we see that $|dh|$ are determined by $|dR|$, k, and R. For a constant $|dR|$ and k, $|dh|$ increases with the decrease of R. Extremely, $|dh| \to |dR|/R^2$ ($R \to 0$). Thus, if we need a constant precision of δ, it will be:

$$|dh| \le \delta \Rightarrow |dR| \le \delta \Big/ \sqrt{\frac{1}{R^4} + \frac{k^2}{R^2}} \,. \tag{10}$$

Then, we can get the number of segments M by:

$$|dR| = \frac{2\pi}{kM} \le \delta \Big/ \sqrt{\frac{1}{R^4} + \frac{k^2}{R^2}} \Rightarrow M \ge \frac{2\pi}{k\delta} \sqrt{\frac{1}{R^4} + \frac{k^2}{R^2}} \,. \tag{11}$$

In fact, (11) is unsolvable for if R=0, the number of segment M=+∞ which is impossible in reality. However, in MoM, to avoid singularity of Green's function, nine-point approximation method is adopted which makes the minimum of R is determined by the minimum length of edges of triangular patches, as shown in Fig. 5. Here, we consider a generalized situation: in most occasions, a sampling rate of $\lambda/10$ is required to ensure the accuracy. It will be:

$$R_{\min} \approx \frac{l}{3} \le \frac{\lambda}{30} \,. \tag{12}$$

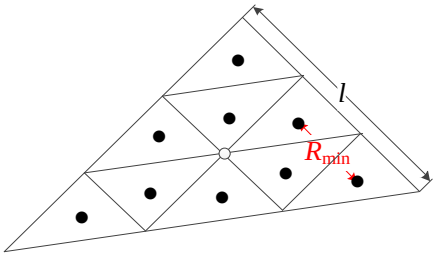

Fig. 5. Sketch map of nine-point approximation.

Substituting $R_{\min}$ into (11), we can get the number of segments M. And in a specific application, $R_{\min}$ can be obtained from the information of triangulations. More significantly, with (11), accuracy of the approach can be controlled which is the main contribution of this work. Having got the number of segments, we can build a value list of Green's function phase item for each segment as shown in Table 1.

Then, if we want to get the value of a specific Green's function, we no longer need to calculate the phase item and can directly get the phase item by searching the value list according to the index in (13) where operator mod(•) represents getting the remainder after division:

$$n = \mathrm{mod}(kR / 2\pi) \,. \tag{13}$$

If n locates in the i-th range of kR, we can directly assign $e^{-jkR} \approx vi$. More importantly, the value list is independent of the problems we are analyzing and is universal for all problems. Thus, we can compute and store it in advance; which is helpful for improving efficiency, especially for large scale problems. For example, in an electromagnetic problem, if there are

N=10^4 RWG functions, the size of impedance matrix will be N^2=10^8. For each couple of RWG functions, Green's functions between them need to be calculated 4 times. Moreover, if nine-point approximation is adopted to avoid singularity, there will be more than 36×10^8 time calculations of Green's functions.

Table 1: A value list for the phase item of Green's function (M_0 is the number of segments)

No.	1	2	…	i	…	M_0
Range of kR	$[0,2\pi/M_0]$	$[2\pi/M_0,4\pi/M_0]$	…	$[2\pi(i\text{-}1)/M_0,2\pi i/M_0]$	…	$[2\pi(M_0\text{-}1)/M_0,2\pi]$
Value	$v1$	$v2$		vi	…	vM_0

III. NUMERICAL RESULTS

To validate efficiency and accuracy of the approach, we compare the elapsed time and approximation errors between direct calculation method and the interpolation scheme with working frequency being f=1 GHz and the number of segments being M_0=1.9×10^7, as shown in Fig. 6 and Fig. 7. And from the results we can see that, the elapsed time of direct calculation method is about 3.5 times of the interpolation scheme with approximation error of the interpolation scheme being less than 10^{-6}.

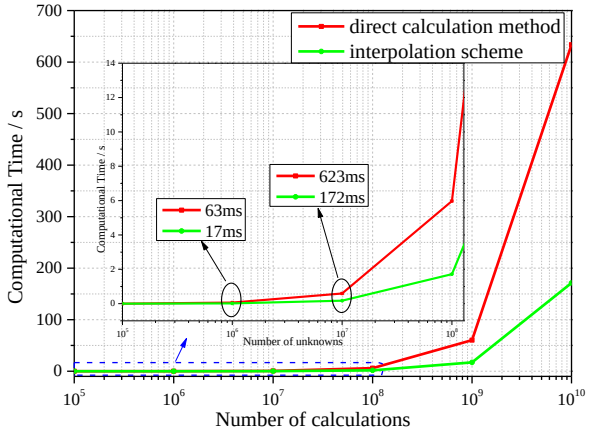

Fig. 6. Changing tendency of computational time varies with the number of calculations. Figures are obtained in a 64-bit personal computer whose dominant frequency is 3.2 GHz.

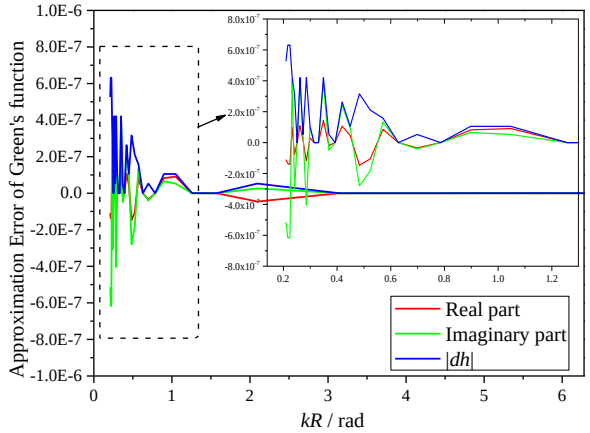

Fig. 7. Approximation error of the interpolation scheme in comparison to direct calculation method.

This demonstrates that the interpolation scheme not only can maintain accuracy but can also improve the efficiency to some extent. Especially, the advantages of the interpolation scheme become bigger with growth of computational scales and this is meaningful for the analysis of large scale problems. More appealing, since the value list of Green's function phase item is built on the basis of kR, it has taken working frequency into consideration which means the value list built for one case can be also reused for other applications. And if we want to get a higher accuracy, we only need to make the value of segments M bigger according to $R_{\min}$.

Then, to further demonstrate efficiency and accuracy of the proposed interpolation scheme, we calculate the elapsed time in filling impedance matrix for a sphere whose radius is 0.3m with working frequency ranging from 0.5 GHz to 2.0 GHz. Figure 8 shows the comparison between direct calculation method and the proposed interpolation scheme. Results exhibit advantages of the proposed interpolation scheme in improving efficiency. Specifically, for 2.0 GHz, the elapsed time of filling impedance matrix is improved about 15% compared to direct calculation method. This may seem not to be very appealing to us. But, it should be noted that, this improvement is obtained only on the calculation of Green's function. And this scheme can be combined with other fast calculation methods such as FMM to further speed up the solution of MoM matrix.

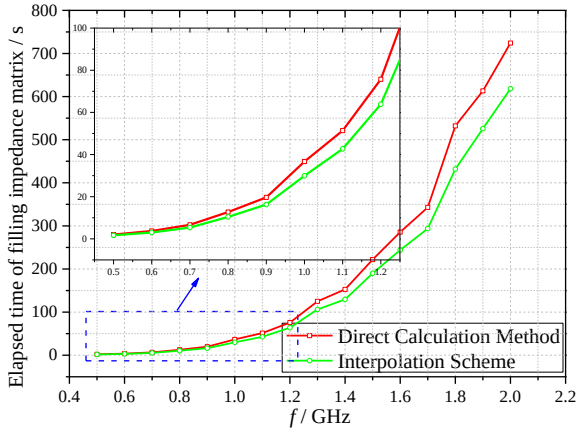

Fig. 8. Elapsed time of filling impedance matrix for a sphere whose radius is 0.3m with working frequency ranging from 0.5 GHz to 2.0 GHz. Sampling rate of triangulation is λ/10.

Moreover, we also compare the impedance matrices calculated by the proposed interpolation scheme and direct calculation method as shown in Fig. 9. From Fig. 9 we know that, in general, discrepancy between the interpolation scheme and direct calculation method is close to 0 dB which reflects that the proposed scheme has a satisfying accuracy.

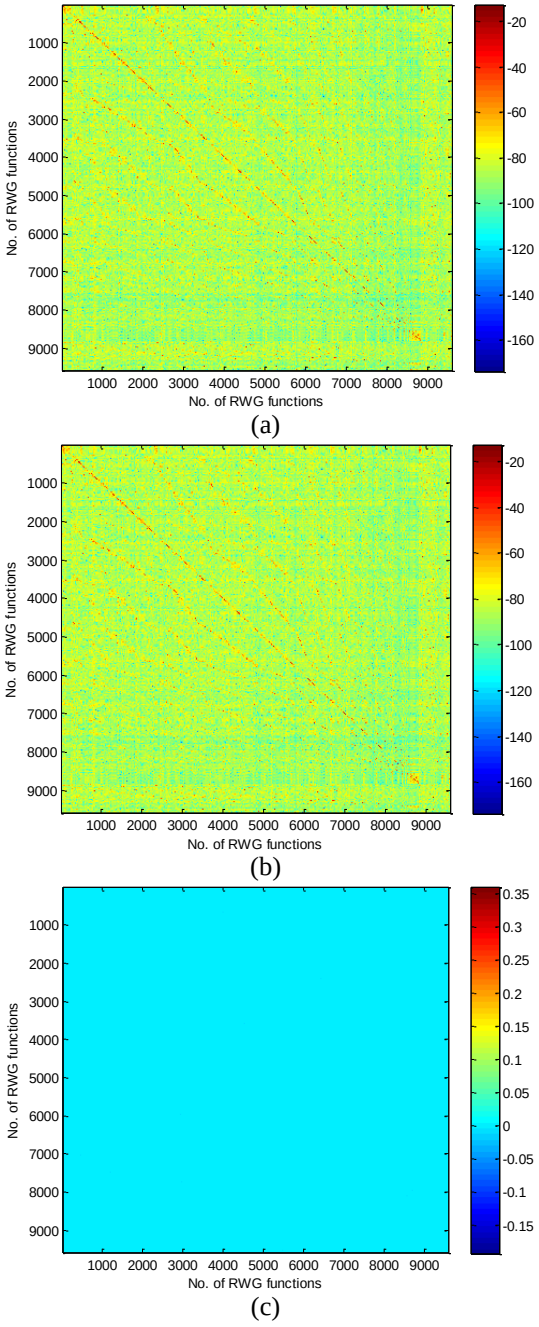

Fig. 9. Impedance matrix ($20\log_{10}|Z|$) of a sphere whose radius is 0.3m with working frequency being 1.25 GHz. (a) Direct calculation method; (b) the interpolation scheme; (c) discrepancy of (a) and (b): $20\log_{10}|Z_a/Z_b|$.

V. CONCLUSION

An interpolation scheme is proposed to accelerate the calculation of Green's function. Through theoretical analysis, we explore the method on how to build a universal value list to ensure a constant accuracy and this is the main contribution of this work. Finally, via numerical examples and the calculation of MoM matrix, accuracy and efficiency of the proposed interpolation scheme is fully validated. Moreover, the scheme is not only limited to the calculation of impedance matrix but also suits for all problems including the calculation of Green's functions.

REFERENCES

[1] C. Tai, *Dyadic Green Functions in Electromagnetic Theory*. 2nd, IEEE Press, 1994.

[2] V. I. Okhmatovski and A. C. Cangellaris, "A new technique for the derivation of closed-form electromagnetic Green's functions for unbounded planar layered media," *IEEE Trans. Antennas Propag.*, vol. 50, pp. 1005-1016, July 2002.

[3] S. M. Jeffrey, J. C. Peter, J. H. Michael, and W. W. Aihua, "A Green's function approach to calculate scattering width for cylindrical cloaks," *Applied Computational Electromagnetics Society*, vol. 25, no. 2, Feb. 2010.

[4] B. Honarbakhsh and A. Tavakoli, "A closed-form spatial Green's function for the thick microstrip substrate: The meshless interpolation approach," *Applied Computational Electromagnetics Society*, vol. 28, no. 2, Feb. 2013.

[5] R. F. Harrington, *Field Computation by Moment Method*. New York: Macmillan, 1968.

[6] N. Engheta, W. D. Murphy, V. Rokhlin, and M. S. Vassilion, "The fast multipole method (FMM) for electromagnetic scattering problems," *IEEE Trans. Antennas Propag*., vol. 40, no. 6, pp. 634-644, June 1992.

[7] J. M. Song and W. C. Chew, "Multilevel fast multipole algorithm for solving combined field integral equations of electromagnetic scattering," *Microwave Opt. Tech. Lett*., vol. 10, no. 1, pp. 14-19, Sep. 1995.

[8] J. M. Song, C. C. Lu, and W. C. Chew, "MLFMA for electromagnetic scattering from large complex objects," *IEEE Trans. Antennas Propag*., vol. 45, pp. 1488-1493, Oct. 1997.

[9] J. M. Rius, J. Parron, E. Ubeda, et al., "Multilevel matrix decomposition algorithm for analysis of electrically large electromagnetic problems in 3-D," *Microwave Opt. Tech. Lett*., vol. 22, no. 3, pp. 15-26, 1999.

[10] K. F. Sabet, J. C. Cheng, and L. P. B. Katehi, "Efficient wavelet-based modeling of printed circuit antenna arrays," *IET Microwave, Antennas & Propagation*, vol. 146, pp. 289-304, 1999.

[11] F. X. Canning, "Improved impedance matrix localization method," *IEEE Trans. Antennas Propag*.,vol. 41, no. 5, pp. 659-667, 1993.
[12] H. H. Hu and Y. F. Sun, "A fast efficient method for computing impedance matrix," *Journal of Hefei University of Technology*, vol. 34, no. 4, Apr. 2011. (In Chinese).
[13] Y. L. Xu, Y. Hu, et al., "Scattering analysis of periodic composite metallic and dielectric structures with synthetic basis functions," *Applied Computational Electromagnetics Society*, vol. 30, no. 10, Oct. 2015.
[14] S. M. Rao, D. R. Wilton, and A. W. Glisson, "Electromagnetic scattering by surfaces of arbitrary shape," *IEEE Trans. Antennas Propag*., vol. AP-30, pp. 409-418, May 1982.
[15] Y. Kamen and L. Shirman, "Triangle rendering using adaptive subdivision," *IEEE Computer Graphics and Applications*, pp. 95-103, Mar.-Apr. 1998.

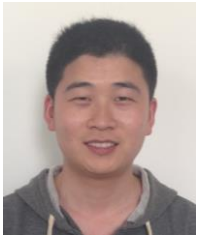

Xu Yanlin was born in Anhui, China, in 1990. He received the B.S. degree in Electronic Engineering from National University of Defense Technology, Changsha, China, in 2013, and is currently pursuing the M.S. degree in Electronic Science and Technology at National University of Defense Technology, Changsha, China.

His research interests include computational electromagnetic and its applications in scattering analysis.

Yang Hu was born in Anhui, China, in 1973. He received the Ph.D. degree in Electronic Science and Technology at National University of Defense Technology, Changsha, China, in 2007, and is currently a Professor of National University of Defense Technology.

Yang has been researching on time domain algorithm and its applications, waveguide slot array antenna, UWB antenna, microstrip antenna etc.

Liu Xiang was born in Hunan, China, in 1972. He received B.S. degree in Electronic Technology from National University of Defense Technology, Changsha, China, in 1994, and received M.S. degree in Electronic and Communication Engineering at National University of Defense Technology, Changsha, China, in 2006. He is currently an Associate Professor in Hunan Institute of Science and Technology, Changsha, China.

His research interests are electronic science and communication engineering.

Rongjun Shen was born in Anhui, China, in 1936. He is a Member of the Chinese Academy of Engineering, China. He is also a Professor with the College of Electronic Science and Engineering, National University of Defense Technology, Changsha, China. His current research interests include air survey and satellite communications.